

URB - Urban Routing Benchmark for RL-equipped Connected Autonomous Vehicles

Ahmet Onur Akman^{*1}, Anastasia Psarou¹, Michał Hoffmann¹, Łukasz Gorczyca¹,
Łukasz Kowalski², Paweł Gora¹, Grzegorz Jamróz¹, Rafał Kucharski¹

¹ Faculty of Mathematics and Computer Science, Jagiellonian University, Kraków, Poland

² Urban Policy Observatory, Institute of Urban and Regional Development, Warsaw, Poland

Abstract

Connected Autonomous Vehicles (CAVs) promise to reduce congestion in future urban networks, potentially by optimizing their routing decisions. Unlike for human drivers, these decisions can be made with collective, data-driven policies, developed by machine learning algorithms. Reinforcement learning (RL) can facilitate the development of such collective routing strategies, yet standardized and realistic benchmarks are missing. To that end, we present URB: Urban Routing Benchmark for RL-equipped Connected Autonomous Vehicles. URB is a comprehensive benchmarking environment that unifies evaluation across 29 real-world traffic networks paired with realistic demand patterns. URB comes with a catalog of predefined tasks, four state-of-the-art multi-agent RL (MARL) algorithm implementations, three baseline methods, domain-specific performance metrics, and a modular configuration scheme. Our results suggest that, despite the lengthy and costly training, state-of-the-art MARL algorithms rarely outperformed humans. Experimental results reported in this paper initiate the first leaderboard for MARL in large-scale urban routing optimization and reveal that current approaches struggle to scale, emphasizing the urgent need for advancements in this domain.

1 Introduction

Recent technological [55] and algorithmic [33] advancements let us believe that in the foreseeable future Connected Autonomous Vehicles (CAVs) will enter our cities and start driving alongside human drivers [42, 66], not only successfully navigating through the traffic complexity and arriving safely at the destination, but also making independent routing decisions: which route to select to reach the destination. A possible future scenario could be as follows: *In a small French town of St. Arnoult, 40% of drivers decide to switch to autonomous driving mode, delegating their routing decisions. Then, either each vehicle or the central controller will apply some algorithm to select routes to minimize travel costs.* This raises a series of significant and open research questions:

1. Which algorithm is most suitable for collective urban fleet routing?
2. Does RL outperform alternative operations research (OR) or machine learning (ML) methods? If yes, how efficient can the training be, what reward formulation best captures the objective, should the solution be centralized or decentralized, how can we formulate useful observations within practical constraints? How detailed environment simulations are needed?
3. How does the problem scale with network complexity, number of agents, and planning horizon?
4. What is the impact of applying such algorithms on: the transportation system, CAVs, and non-CAV drivers? By focusing only on algorithmic goals, are we overlooking any significant aspects of CAV deployment that may be detrimental to our urban societies (increased emissions, mileage, variability, inequality, etc.)?

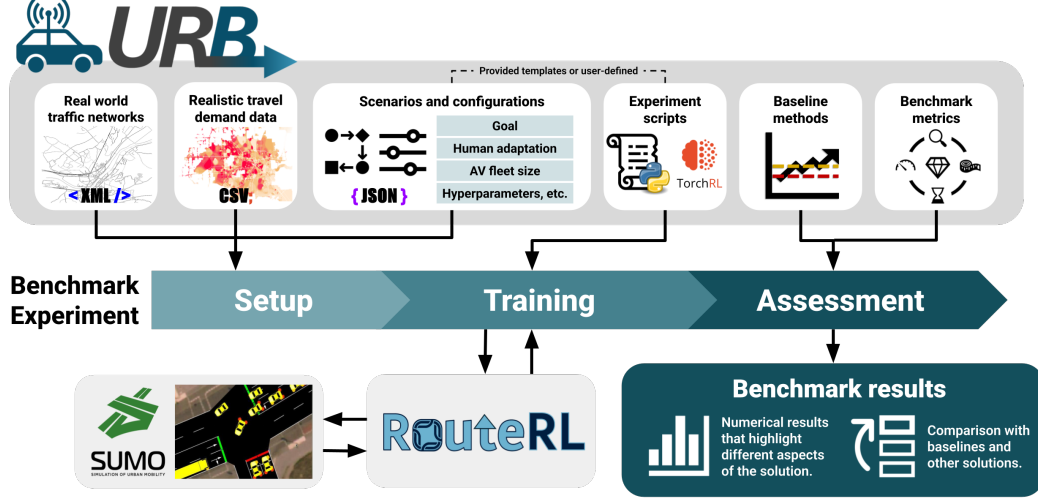


Figure 1: URB is a comprehensive benchmarking framework for MARL methods in solving CAV routing tasks in a mixed urban traffic environment. It enables end-to-end assessment through a collection of 29 real-world traffic networks, realistic demand patterns, baseline methods, domain-specific performance indicators and a flexible parameterization scheme.

Those questions are timely, yet open [50, 31]. Therefore, in this study, we introduce URB - a comprehensive benchmarking framework for MARL methods in solving CAV routing tasks in a mixed (CAV-human) urban traffic environment. We outline its motivation, theoretical foundation, design, and key features. We then initiate the first URB leaderboard of the four most established MARL algorithms on a representative scenario and document how each solution affects different system efficiency statistics. Finally, we discuss URB’s practical potential and limitations, and outline the future directions we intend to pursue.

The human-CAV urban routing problem is interdisciplinary and intersects traffic engineering, with detailed vehicle dynamics and traffic flow properties, transport engineering, with day-to-day route choice behavior in human daily demand patterns, and machine learning, with a discrete optimization problem on a huge action space in a non-stationary environment. URB bridges experts from the above fields, allowing them to contribute without in-depth domain expertise. In particular, thanks to SUMO [38] integration and interface of the common human route choice models and demand patterns, machine learning researchers can test their custom algorithms on realistic traffic scenarios. Likewise, transport researchers, thanks to the provided TorchRL [7] implementations, may use state-of-the-art RL algorithms and test their impact on custom traffic and travel demand scenarios.

With URB we aim to trigger positive competition within the RL community to propose new algorithms, and test them on a diverse set of tasks and instances. Hopefully, URB leaderboard will eventually be dominated by efficient, scalable, reliable and socially aware solutions that, when deployed in real networks, will improve the performance of all the parties involved. URB will be gradually extended with problems that will arise in the future, when CAVs will start operating in our cities in various configurations, with candidate solutions (from within the RL community and outside) evaluated on a wide set of measures and problem instances. This is particularly timely before CAV fleets are deployed, to inform the society about potential threats and motivate vehicle developers to propose sustainable fleet operating algorithms.

URB’s codebase¹ and data collection² are publicly available in online repositories under non-restrictive licenses, as detailed in Appendix C.1.

¹<https://github.com/COeXISTENCE-PROJECT/URB>

²<https://doi.org/10.34740/kaggle/ds/7406751>

1.1 Urban routing and (MA)RL - significance and challenges calling for benchmark

The urban routing problem with CAVs is not only *significant* for future societies, but also *challenging*. The CAVs promise to relieve our congested networks by enabling a new class of routing behaviors, potentially making better use of scarce resources (capacity) for better global and user-level performance. This translates into minutes saved daily and hours saved annually for all commuters, and tons of fuel and CO₂ emissions saved at the system level.

Realizing this potential, however, requires solving a highly non-trivial problem. With thousands of agents (up to millions in megacities) taking simultaneous actions in large action spaces (here we sample only a few routes, while the choice set grows exponentially with network size), the environment is not only non-deterministic (due to the stochastic nature of traffic and the heterogeneity of people), but also non-stationary (as agents compete for limited resources in a game-like fashion) and costly to simulate. One environment run can take up to hours (with detailed simulators like SUMO) in real-size cities, while MARL algorithms often require millions of training episodes. At the same time, standard discrete OR techniques fail in such large action spaces [41].

Existing studies applied MARL to tackle the urban routing problem. In [61], drivers use MARL with different rewards to minimize congestion, but consider only homogeneous agent populations and global reward; in [51], authors proposed a regret-minimization for MARL route selection with external traffic data, and [59] used a centralized controller with a simplified macroscopic traffic simulation. Here, we build on it and extend, testing and simulating diverse scenarios and solutions in RouterL [2], a MARL environment integrated with a microscopic traffic simulator, SUMO.

In line with the aforementioned studies, we argue that solving the urban routing problem with RL may be the most intuitive direction, as it can be naturally reframed as a decision-making task, and the optimization target can be intuitively formulated as a reward signal. The human day-to-day route-choice learning process [67] naturally resembles the classical RL training loop. RL facilitates experience-driven learning and adaptability, which are particularly useful for complex, large-scale, and dynamic problems. Moreover, existing RL research introduced approaches that could potentially address the challenges involved in the urban route choice problems, such as managing a large group of agents [10, 8], communication mechanisms [69, 62], and developing network-agnostic routing strategies [5, 44]. Moreover, multi-agent learning may be an effective way to decompose this large-scale optimization problem into smaller learning tasks.

Nonetheless, as our results suggest, the current frontiers of MARL algorithms fall short of addressing the problem complexities. To this end, we introduce a unified ground to stimulate advancements in this domain, similarly to other successful traffic-related RL benchmarks like FLOW [32], RESCO [4], or [63]. We are optimistic that the RL community, challenged by URB will propose reliable, generalizable, and efficient solutions. To the best of our knowledge, no existing benchmark or RL environment combines all the mentioned characteristics into a single problem instance; thus, solving it will support the general MARL development and benefit any other domain where MARL is applicable.

2 Background

2.1 Urban routing problem

We consider a specific variation of the classic traffic assignment problem (TAP) [11] (known in game theory as a repeated congestion game [20]) to represent the actual commuting decisions made by drivers in congested urban traffic networks every day worldwide. Each agent (driver) selects the subjectively optimal route to reach their destination at minimal cost [45]. Agents' decisions, due to limited capacity, contribute to system travel costs (congestion). The demand (agents with their origins, destinations, and departure times) is fixed. Every day (later formalized as an RL episode), they update their knowledge with the recent experience and select the subjectively optimal routes [70]. Such a system is expected, after sufficient learning, to reach the so-called User Equilibrium, which is stable [40], a specific version of Nash Equilibrium [65], where none of the drivers may improve payoffs (here, simply the travel time) by unilaterally switching a route. This, however, relies on very strict conditions (perfect rationality and knowledge about the traffic conditions [9]) that are not met in practice, so real-world conditions (as well as microscopic agent-based models resembling them) only approximate the equilibrium conditions.

In URB, the realistic microscopic traffic simulator SUMO is used to reproduce travel costs (here, simply the travel times) and a Markov learning model is used to update knowledge, on which each human driver makes subjectively optimal routing decisions [18]. In brief, every day τ , each agent i executes an action $a_{i,\tau}$ from the set of routes K_i , to maximize own expected utility U (reward, here simply the negative travel time) $a_{i,\tau} = \arg \max_{k \in K_i} U_{i,\tau,k}$ (where K_i is the set of possible agent's i routes). Daily, the agent i updates own expectations with recent experienced travel time $t_{i,\tau,k}$: $U_{i,\tau,k} = HLM(U_{i,\tau-1,k}, t_{i,\tau,k})$. Details for Human Learning Model (HLM) are provided in Appendix D.3. In this research, we use the standard yet stable and reproducible model to isolate the impact of algorithms from non-deterministic, heterogeneous, and suboptimal travel behavior (also available from RouteRL).

2.2 Urban routing problem with autonomous vehicles

While the above problem has been present since the first traffic jams in our cities and is well studied, its new formulation [2], where limited resources of urban traffic networks are shared between CAVs and human-driven vehicles, is less known. When autonomous vehicles, rather than humans, decide how to reach a destination, the problem changes significantly: (i) instead of making behavioral routing decisions, CAVs seek optima algorithmically, (ii) instead of subjectively perceived costs, CAVs have predefined reward functions, (iii) which, unlike for humans, can go beyond their own travel time and (iv) can become shared and potentially collective.

2.3 Problem formulation

During several consecutive episodes (days of commute τ), each agent (vehicle i) makes a pre-trip routing decision a_i^τ , i.e., chooses from the precomputed set of routes based on the observed state. Humans $i \in \mathcal{N}_{HDTV}$ use the behavioral model explained above, while CAVs $j \in \mathcal{N}_{CAV}$ use their routing policies π to select an action a in a given (observed) state o : $a \sim \pi(a|o)$. Agent rewards (from travel times yielded by SUMO) depend on the joint actions of all agents. In URB, we typically consider scenarios where: (1) humans train first and stabilize their action probabilities, followed by (2) the mutation where some agents become CAVs and (3) start training by applying some learning algorithm to maximize a reward signal, and finally (4) in the testing phase, they do not learn and roll out trained policies for several days (episodes).

We follow [2] and formalize this problem as the Agent-Environment Cycle (AEC) game [58], where in each episode, agents \mathcal{N} , either human or CAV, in order v of departure time, select a route from their action space. Within the episode, the system evolves according to traffic dynamics (P simulated with SUMO) and actions (i.e., route choices) of all agents. The detailed snapshot of the traffic system is the state $s \in S$, part of which agents may observe before acting. At the end of the episode, SUMO yields individual travel times, from which the reward is calculated.

This can be formalized as:

$$\langle S, \mathcal{N}, (A_i)_{i \in \mathcal{N}}, P, (R_i)_{i \in \mathcal{N}}, (O_i)_{i \in \mathcal{N}}, v \rangle,$$

Where:

- **State space S :** Global state $s \in S$ encodes all relevant information about the traffic system in a given timestep, including the status of traffic lights, routes chosen by agents with earlier departure times, active vehicles, and their attributes (e.g., their trajectories, velocities, locations). States are not observable to the agents, so they receive only observation signals $o_i \in O_i$.
- **Agent set \mathcal{N} :** Human drivers and CAVs with predefined origins, destinations, and departure times.
- **Action spaces $(A_i)_{i \in \mathcal{N}}$:** Set of K_i precomputed routes connecting the agent i 's origin and destination: $A_i = \{0, \dots, K_i - 1\}$.
- **Transition function P :** It is a result of interplay between the agents actions (i.e. route choices) and the dynamics of the traffic flow (in URB simulated with SUMO), which updates the global state S at every timestep by progressing the vehicles along their routes towards destination according to the network topology and Intelligent Driver Model (IDM) implemented in SUMO [60].
- **Reward functions $(R_i)_{i \in \mathcal{N}}$:** They are computed for each agent from individual travel times at the end of the episode. For human drivers, it is the (negative) travel time. For CAVs, it can be any linear combination of own, group, and system travel time statistics. The parameterization of this

combination models the CAV behavior, which can be selfish, social, altruistic, malicious, etc. (see [54] for classification of CAV behaviors).

- **Observation functions** $(O_i)_{i \in \mathcal{N}}$: It is assumed that each CAV agent, before making a routing decision, receives information about the route choices made in the current episode by agents whose departure times are earlier than the departure of the observing agent. Meanwhile, human agents make decisions solely based on their cost expectations (see Appendix D.3).
- **Agent selection mechanism** v : Agents act sequentially following a fixed schedule defined by v , which enforces a temporal order based on agent departure times within an episode.

Such formulation allows us to apply a wide variety of methods (not only MARL algorithms). Additionally, it offers flexibility in the task formulation (e.g., in the reward, observation, or learning loop) to cover most relevant instances of URB problems. Unlike Markov Decision Process (MDP) and Partially Observable Stochastic Game (POSG) models (as used in [56, 59, 13]), AEC, within the turn-based structure, provides an intuitive interface for implementing a decision-making process based on partial observations of real-time traffic conditions.

2.4 Multi-agent reinforcement learning algorithms

We benchmark four promising state-of-the-art MARL algorithms, applicable to discrete action space scenarios and common in baselines or building blocks of more complex algorithms [19, 16, 49, 64, 71, 52]. For investigating the properties of solutions found by different classes of algorithms, we use two *independent learning* (IL) algorithms, where each agent learns separately and treats the other agents as part of the environment, and two algorithms with the *Centralized Training Decentralized Execution* (CTDE) property [3], where agents learn decentralized policies from local observations while collectively maximizing a shared global objective using global state information in centralized training. IL introduces non-stationarity from the perspective of each agent, often resulting in a lack of convergence guarantees in multi-agent settings [57], yet typically requires less computational resources and is easier to scale to large environments [36]. CTDE, on the other hand, helps address the non-stationarity that arises in the IL case [72].

- **Independent Q-Learning (IQL)** [57] is a value-based IL algorithm where each agent trains its own deep Q network. It is a useful reference point as it often works well in practice; nevertheless, it lacks theoretical convergence guarantees [17, 39].
- **Independent Proximal Policy Optimisation (IPPO)** [14] is an actor-critic method that has empirically shown to be effective in a variety of tasks [68, 49].
- **Multi-Agent PPO (MAPPO)** [68] is an actor-critic algorithm that utilizes a centralized critic (in contrast to IPPO). It is considered a competitive baseline for cooperative MARL tasks.
- **QMIX** [53] employs a mixing network to decompose the joint state-action value function. QMIX is a *Value Decomposition* method, designed for fully cooperative tasks, where all agents share a common reward. Value decomposition methods learn a centralized joint state-action value function and factorize it into individual agent-specific value functions to enable decentralized execution while attributing each agent’s contribution to the collective reward.

3 Urban Routing Benchmark - URB

URB is a collection of real-world traffic networks and associated realistic demand patterns, paired with reusable experiment scripts and a parameterization scheme. A URB experiment can be specified and initialized with a simple command:

```
python scripts/<script_name> --id <exp_id> --alg-conf <hyperparam_id>
--env-conf <env_conf_id> --task-conf <task_id> --net <net_name>
--env-seed <env_seed> --torch-seed <torch_seed>
```

Above:

- `<script_name>` points to the algorithm implementation, which may be one of our baselines, provided TorchRL scripts, or custom.
- `<id>` is the unique experiment identifier.

- `<hyperparam_id>`, `<env_conf_id>`, and `<task_id>` control the algorithm hyperparameterization, experiment settings (e.g., action space, disk operations), and task specifications (e.g., the share of CAVs and their reward), respectively.
- `<net_name>` is the name instance (network graph and corresponding demand pattern).
- `<env_seed>` and `<torch_seed>` control the reproducibility of the environment and training, respectively.

Training records and plots are saved in `results/<exp_id>`. We document the installation and usage of URB in Appendix C.3.

URB is integrated with the ML and transportation standard tools and libraries. This is done mainly via the RouteRL [2] integration, which is a framework that integrates MARL with a microscopic traffic simulation for our day-to-day route-choice learning problem. RouteRL simulates the daily route choices of driver agents in a city, including two types: human drivers and CAVs. The integrated microscopic traffic simulator, SUMO, reproduces how individual vehicles traverse the complex traffic networks [38]. SUMO (detailed in Appendix D.2) is a standard in the open-source community, with very few alternatives, despite its limitations (quite heavy, written in C, and single-threaded). The input is the standard CSV files, OpenStreetMap graphs [47], and JSON editable configuration file. For route generation, we use our implementation of Dial-like route generator *JanuX* [1] (detailed in Appendix D.4).

Problem instance: Road network and demand pattern URB task is executed on a given network with a given demand pattern. URB is shipped with traffic networks of 28 Île-de-France subregions and Ingolstadt (from RESCO). Apart from the road networks, URB comes with realistic trip demand patterns associated with each network, in the format of sets of agents defined with their origins, destinations, and departure times (we use AM peak from daily demand data). We use external demand patterns (like [4] for Ingolstadt) or a synthetic demand generation pipeline based on empirical data (like [22] for 28 Île-de-France networks). The set of simulated agents is stored in the readable `agents.csv` files within the provided dataset. More details on network extraction and demand generation are documented in Appendix A. The three traffic networks, which are used in *Scenario 1* reported in Section 4, are visualized in Figure 2. We also provide the visualizations and demand statistics associated with each network included in URB in Appendix E.

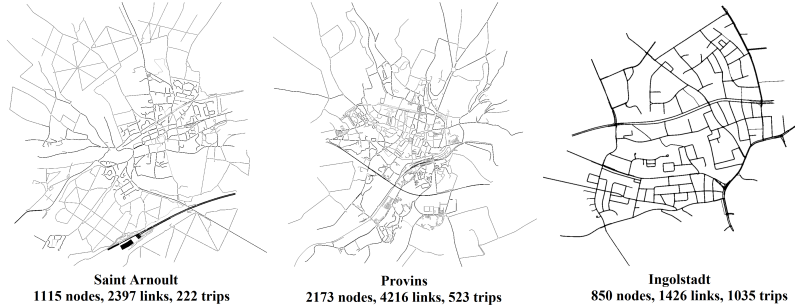


Figure 2: Three traffic networks we use in our benchmarking study (Section 4), shown in order of increasing demand levels: (a) St. Arnoult (small), (b) Provins (medium) and (c) Ingolstadt (large; from RESCO traffic light benchmark [4]).

URB training pipeline: A typical task starts with a few hundred days of human learning, where each episode is treated as a single day of commute. This is followed by a *mutation* where a given share of vehicles become CAVs. Then, humans do not learn (but act according to already learned policies), and the CAVs start training - here, episodes are virtual and do not necessarily have physical meaning. Finally, we run rollouts to showcase learned routing strategies, where both groups of agents follow their fixed policies for choosing their routes. See details in [2] and in the Appendix D.1.

Scenarios To thoroughly test candidate strategies, URB facilitates experimenting with a wide range of route-choice tasks. URB is modular and highly customizable, with a parameterization scheme allowing configuration of:

- **Algorithms:** Off-the-shelf and custom implementations (including TorchRL’s modular components for building policies, value functions, and losses, as well as multi-agent implementations where agent policies can be centralized or decentralized and agents may share information).
- **Network topology:** One of 29 real-world traffic networks and associated demand data, varying in graph size and congestion, to test generalization and scalability as problem complexity increases.
- **CAV market share:** Fraction of agents that become CAVs, which can range from 0 up to 100% of agents.
- **CAV behavior profile:** Users can choose the objective to be pursued by the CAV fleet. These behaviors (as mentioned in Section 2.3) allow assessing the different social and ethical consequences of CAV deployment.
- **Human learning model:** Users can choose and parameterize the human learning model according to the driver behavior they wish to model in a given city. The possible parameterizations can yield greedier or more random human drivers’ behaviours.
- **Action spaces:** Users can set the choice set size (number of routes).
- **Length and phases of the experiment and hyperparameterization** for the selected algorithm.

Evaluation metrics The core metric is the travel time t , which is both the core term of the utility for human drivers (rational utility maximizers) and of the CAVs’ reward. To compare the general impact of the autonomous fleet on the system we calculate the average times over all agents (t^{pre} , t^{train} , t^{test}) during periods of human learning, fleet training and policy testing, respectively. The t_{CAV} and t_{HDV} are times of CAVs and human drivers, respectively. We measure the *cost of training*, expressed as: $c_{\text{all}} = \sum_i \sum_{\tau \in \text{train}} (t_i^\tau - t_i^{\text{pre}}) / (|\mathcal{N}| \cdot |\text{train}|)$, where t_i^τ is the time of agent i in episode τ and t_i^{pre} is the average experienced time of agent i for the last 50 days before CAVs are introduced. Similarly, we introduce c_{HDV} and c_{CAV} for respective groups of agents. To better understand the causes of the changes in travel time, we track the changes in mean speed $\Delta_v < 0$ and mileage $\Delta_L > 0$ (directly extracted from SUMO) for the policy testing period. The winrate **WR** is the percentage of experiment runs where CAVs, after training, reached shorter mean travel times than humans ($t_{\text{CAV}} < t^{\text{pre}}$).

Baselines URB includes naive baseline methods for the route choice problem for groundedness in the benchmarking tasks. **All-or-Nothing** (AON) model deterministically selects the route with the minimal free-flow time, where free-flow time is the expected travel duration under zero congestion. **Random** model selects an action randomly with a uniform probability. The **human** baseline assumes that CAVs replicate human routing decisions (apply trained human model).

4 Results

We report the result of the most representative scenario (out of multiple possible with URB) performed on three instances (cities), complemented with sample results from alternative scenarios.

Scenario 1: In a given network with a fixed demand pattern, experienced human agents have learned their route-choice strategies (minimized travel times). At some point, a given share of them *mutate* to CAVs and delegate routing decisions. Then, for a given number of training episodes, the agents develop routing strategies to minimize their delay using MARL.

It is executed with a 40% share of CAVs on three networks (Figure 2). The human stabilization and CAV training take 200 and 6000 episodes, respectively, followed by 100 testing (non-learning) episodes. We use cooperative reward (minimize group travel time) for cooperative algorithms (MAPPO, QMIX) and selfish reward (minimize own travel time) for IL algorithms (IQL, IPPO). We visualize and assess (using URB metrics) our results in Figure 3 and Table 1, respectively. All experiment parameterizations and computation times are detailed in Appendix B.

The learning of IQL exhibits the well-known instability issues of IL settings [46]. IPPO shows gradual improvements, indicating the previously explored effectiveness of value-clipping and on-policy updates for non-stationarity [68] over IQL. Nonetheless, both IL algorithms fail to achieve near-human performance, with increasing gaps in saturated networks. MAPPO and QMIX utilize centralized training mechanisms with shared objectives (cooperative reward). MAPPO learning is inefficient and worsens with the increasing fleet size. We hypothesize that this is the result of the difficulty in handling the large global information with a centralized critic [68]. For QMIX, CAVs

beat the human baseline in 2/3 of experiment runs in St. Arnould. Interestingly, QMIX exhibits abrupt performance jumps. This aligns with the prior empirical findings with how every agent switches their expectations at once when the QMIX hyper-network’s non-negative weights realign the monotonic mixing so a different joint action maximizes Q_{tot} , and steep drops occur when the same max-operator inflates over-estimated per-agent Q values [48]. The extended training with QMIX does not improve the effectiveness, often converging to comparable results. Notably, in all cases, the human travel times increased after the CAV deployment.

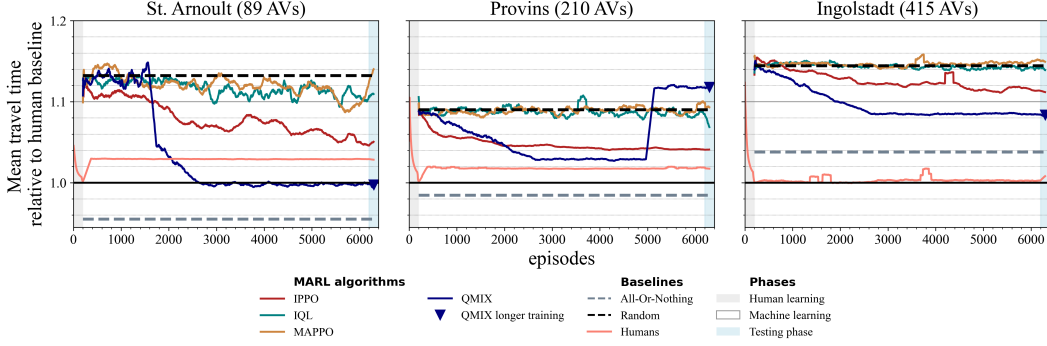


Figure 3: Travel times relative to human baseline (t^{pre}) across episodes in 3 instances (222 to 1035 drivers) in Scenario 1. Baselines are marked with dashed lines, human travel times with a solid black line, and four tested RL algorithms with color lines. We pick the best out of three runs. Algorithms are trained for 6 000 episodes (days simulated in SUMO), and we conduct an additional training with QMIX (as the most promising) for 20 000 (blue triangle). Many algorithms hardly beat the random baseline. In Provins and Ingolstadt, none of the algorithms beat the human baseline, and only QMIX on the smallest instance (St. Arnould) managed to outperform human travel times (in 2 out of 3 runs).

To complement, we investigated what happens when *all drivers in St. Arnould are replaced by CAVs*. Figure 4 depicts the mean travel time changes of the CAV fleet, trained with the same algorithms and parameterizations (for performance metrics see Appendix F.1). Similar to Scenario 1, many algorithms oscillate near random baseline performance; none of the algorithms beat the All-or-Nothing solution. This suggests that the aforementioned issues may also persist in CAV-only systems, extending the scope of the identified methodological shortcomings to a greater variety of future traffic scenarios.

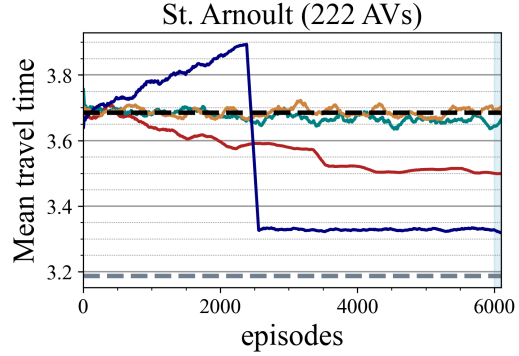


Figure 4: Mean travel times (in minutes) across episodes in St. Arnould for Scenario 2 with CAVs only (for legend consult Figure 3).

5 Conclusions, limitations, broader impact and future work

In this paper, we introduced a benchmark for testing RL routing algorithms in city-scale networks and populated it with TorchRL implementations of a selection of standard MARL algorithms.

Some of its **limitations** are: i) The driving model is the same for humans and CAVs; we intentionally neglect the promised traffic flow improvements of CAVs to isolate their impact on route-choice only. ii) The routes are chosen by agents once per episode. An even more challenging scenario would involve adjusting the route dynamically, rendering it a multiple decision (in contrast to one per episode) setting. iii) The demand is fixed concerning OD pair and departure times, while in real cities, this is not the case. This would add noise to the environment and render it even less stationary. iv) We consider a single CAV fleet, while multiple competing providers are equally possible in the future. Finally, v) an experimental scheme is limited and ought to be widened (to cover more scenarios,

Table 1: Scenario 1 results for three cities (best of 3 runs is reported). Not only do the CAVs experience a longer travel time t_{CAV} than in the human-only system t^{pre} , but the human agents (t_{HDV}) are also disadvantaged by the CAV deployment. The training costs c are significant for all the instances, and overall network performance decreased (lower mean speed: $\Delta_v < 0$ and increased mileage: $\Delta_L > 0$). Out of all algorithms, QMIX was the best. In St. Arnoult, it outperformed humans, while in Provins, it performed even worse than the random baseline. IQL and MAPPO failed to converge and reached performance nearly at random in all instances. The percentage of runs where the CAV fleet outperformed humans **WR** was unsatisfactory. The best for each metric is underlined, while the best RL algorithm is **bolded**.

NET	ALGORITHM	t^{PRE}	t^{TEST}	t_{CAV}	t_{HDV}	c_{ALL}	c_{HDV}	c_{CAV}	Δ_v	Δ_L	WR
ST. ARNOULT	IPPO	3.15	3.28	3.34	3.24	0.6	0.12	1.33	-0.31	0.05	0%
	IQL	3.15	3.34	3.49	3.24	0.66	0.14	1.44	-0.42	0.08	0%
	MAPPO	3.15	3.32	3.43	3.25	0.66	0.14	1.45	-0.27	0.08	0%
	QMIX	3.15	3.2	3.12	3.25	0.65	0.13	1.43	-0.2	0.01	66%
	HUMAN	3.15	3.15	N/A	<u>3.15</u>	0.0	0.0	0.0	0	0.0	100%
	AON	3.15	<u>3.15</u>	<u>3.01</u>	3.25	<u>0.55</u>	<u>0.09</u>	<u>1.21</u>	<u>-0.06</u>	<u>-0.0</u>	100%
	RANDOM	3.15	3.38	3.58	3.25	0.6	0.09	1.36	-0.33	0.1	0%
PROVINS	IPPO	2.8	2.88	2.92	2.85	0.53	0.26	0.93	-0.4	0.03	0%
	IQL	2.8	2.92	3.03	2.84	1.48	0.98	2.23	-0.52	0.06	0%
	MAPPO	2.8	2.92	3.03	2.85	1.23	0.81	1.87	-0.64	0.06	0%
	QMIX	2.8	2.96	3.14	2.85	0.88	0.54	1.41	-0.8	0.07	0%
	HUMAN	2.8	<u>2.8</u>	N/A	<u>2.8</u>	0.0	0.0	0.0	0.0	0.0	100%
	AON	2.8	2.81	<u>2.76</u>	2.84	<u>0.47</u>	<u>0.19</u>	0.99	<u>-0.14</u>	<u>-0.0</u>	100%
	RANDOM	2.8	2.93	3.04	2.85	0.51	0.22	0.95	-0.62	0.06	0%
INGOLSTADT	IPPO	4.21	4.4	4.72	4.18	1.76	1.22	2.56	-0.37	0.07	0%
	IQL	4.21	4.45	4.8	4.22	1.68	1.08	2.59	-0.62	0.07	0%
	MAPPO	4.21	4.44	4.81	<u>4.2</u>	1.82	1.21	2.75	-0.62	0.07	0%
	QMIX	4.21	4.36	4.55	4.23	1.2	0.67	1.98	-0.73	0.02	0%
	HUMAN	4.21	<u>4.21</u>	N/A	4.21	0.0	0.0	0.0	0.0	0.0	100%
	AON	4.21	4.29	<u>4.37</u>	4.23	<u>0.87</u>	<u>0.55</u>	<u>0.24</u>	-0.45	<u>-0.01</u>	0%
	RANDOM	4.21	4.45	4.81	4.22	0.99	0.49	1.74	-0.68	0.07	0%

algorithms, and instances) and deepened (to better tailor the most promising algorithms for this problem).

Solving the urban routing problem by CAVs may have a **broader societal impact** such as: i) Potentially reduced travel times, congestion, and emissions if the developed algorithms are used properly. ii) Undesirable use by CAV operators to boost profits while exploiting human drivers. iii) Deterioration of driving conditions for human drivers in cities if the algorithms are not designed or used cautiously. iv) Pressure on human drivers to join commercial collective routing schemata as independent driving becomes inefficient.

The **future work** could encompass i) Extending the benchmark by addressing the issues raised in the limitations above. ii) Improving implementations of RL algorithms and developing alternative RL and non-RL algorithms to challenge the benchmark leaderboard. iii) Identification of the fundamental reasons why some algorithms performed poorly in certain settings to improve them and advance the RL theory.

Predicting the future of autonomous driving is not an easy task. The safety issues being the most urgent concern, once they are solved, higher-level considerations such as collective routing may become important. Recognizing it, we hope that the presented benchmark will contribute to reducing the uncertainty related to the introduction of fleets of CAVs on a large scale and preempting and mitigating any problematic scenarios this may involve.

Acknowledgement This research is financed by the European Union within the Horizon Europe Framework Programme, ERC Starting Grant number 101075838: COeXISTENCE.

References

- [1] Ahmet Onur Akman. Janux, 2025.
- [2] Ahmet Onur Akman, Anastasia Psarou, Łukasz Gorczyca, Zoltán György Varga, Grzegorz Jamróz, and Rafał Kucharski. Routerl: Multi-agent reinforcement learning framework for urban route choice with autonomous vehicles. *arXiv preprint arXiv:2502.20065*, 2025.
- [3] Christopher Amato. An introduction to centralized training for decentralized execution in cooperative multi-agent reinforcement learning, 2024.
- [4] James Ault and Guni Sharon. Reinforcement learning benchmarks for traffic signal control. In *Thirty-fifth Conference on Neural Information Processing Systems Datasets and Benchmarks Track (Round 1)*, 2021.
- [5] Jacob Beck, Risto Vuorio, Evan Zheran Liu, Zheng Xiong, Luisa Zintgraf, Chelsea Finn, and Shimon Whiteson. A survey of meta-reinforcement learning, 2024.
- [6] Michael Behrisch, Laura Bieker, Jakob Erdmann, and Daniel Krajzewicz. Sumo—simulation of urban mobility: an overview. In *Proceedings of SIMUL 2011, The Third International Conference on Advances in System Simulation*, pages 63–68, 2011.
- [7] Albert Bou, Matteo Bettini, Sebastian Dittert, Vikash Kumar, Shagun Sodhani, Xiaomeng Yang, Gianni De Fabritiis, and Vincent Moens. TorchRL: A data-driven decision-making library for PyTorch. 2023. Publisher: [object Object] Version Number: 2.
- [8] Tianshu Chu, Jie Wang, Lara Codecà, and Zhaojian Li. Multi-agent deep reinforcement learning for large-scale traffic signal control. *IEEE Transactions on Intelligent Transportation Systems*, 21(3):1086–1095, 2020.
- [9] José R Correa and Nicolás E Stier-Moses. Wardrop equilibria. *Encyclopedia of Operations Research and Management Science*. Wiley, 2011.
- [10] Kai Cui, Anam Tahir, Gizem Ekinci, Ahmed Elshamhory, Yannick Eich, Mengguang Li, and Heinz Koeppl. A survey on large-population systems and scalable multi-agent reinforcement learning, 2022.
- [11] Carlos F Daganzo and Yosef Sheffi. On stochastic models of traffic assignment. *Transportation science*, 11(3):253–274, 1977.
- [12] data.gouv.fr. Base sirene – fichier stocketablisement utf8. <https://www.data.gouv.fr/fr/datasets/base-sirene-des-entreprises-et-de-leurs-etablisements-siren-siret/>. Accessed: 2024-12-12.
- [13] Thiago B. F. de Oliveira, Ana L. C. Bazzan, Bruno C. da Silva, and Ricardo Grunitzki. Comparing multi-armed bandit algorithms and q-learning for multiagent action selection: a case study in route choice. In *2018 International Joint Conference on Neural Networks (IJCNN)*, pages 1–8, 2018.
- [14] Christian Schroeder de Witt, Tarun Gupta, Denys Makoviichuk, Viktor Makoviychuk, Philip H. S. Torr, Mingfei Sun, and Shimon Whiteson. Is Independent Learning All You Need in the StarCraft Multi-Agent Challenge?, 2020. Version Number: 1.
- [15] Robert Barkley Dial. *Probabilistic assignment: a multipath traffic assignment model which obviates path enumeration*. University of Washington, 1970.
- [16] Yali Du, Lei Han, Meng Fang, Ji Liu, Tianhong Dai, and Dacheng Tao. Liir: Learning individual intrinsic reward in multi-agent reinforcement learning. In H. Wallach, H. Larochelle, A. Beygelzimer, F. d'Alché-Buc, E. Fox, and R. Garnett, editors, *Advances in Neural Information Processing Systems*, volume 32. Curran Associates, Inc., 2019.
- [17] Jakob N. Foerster, Nantas Nardelli, Gregory Farquhar, Philip H. S. Torr, Pushmeet Kohli, and Shimon Whiteson. Stabilising experience replay for deep multi-agent reinforcement learning. *CoRR*, abs/1702.08887, 2017.

- [18] Christian Gawron. *Simulation-based traffic assignment*. PhD thesis, Universität zu Köln, 1998.
- [19] Peter Henderson, Riashat Islam, Philip Bachman, Joelle Pineau, Doina Precup, and David Meger. Deep reinforcement learning that matters. *CoRR*, abs/1709.06560, 2017.
- [20] Ron Holzman and Nissan Law-Yone. Strong equilibrium in congestion games. *Games and economic behavior*, 21(1-2):85–101, 1997.
- [21] Sebastian Hörl and Kay W. Axhausen. Relaxation-discretization algorithm for spatially constrained secondary location assignment. In *Proceedings of the 99th Annual Meeting of the Transportation Research Board*, Washington, D.C., January 2020.
- [22] Sebastian Hörl and Milos Balac. Synthetic population and travel demand for paris and île-de-france based on open and publicly available data. *Transportation Research Part C: Emerging Technologies*, 130:103291, 2021.
- [23] IGN. Contours iris 2-1 shp (lamb93) – édition 2017. <https://geoservices.ign.fr/documentation/diffusion/telechargement-donnees-libres.html#contoursiris>, 2017. Accessed: 2024-12-12.
- [24] IGN. Bd topo® décembre 2020 – adresses (shp, Île-de-france). <https://geoservices.ign.fr/documentation/diffusion/telechargement-donnees-libres.html#bd-topo>, 2020. Accessed: 2024-12-12.
- [25] INSEE. Population totales 2015 (france hors mayotte). <https://www.insee.fr/fr/statistiques/3627376>, 2015. Accessed: 2024-12-12.
- [26] INSEE. Recensement des personnes localisées au canton ou ville – zone a, recensement de la population 2015 (dbase). <https://www.insee.fr/fr/statistiques/3625223>, 2015. Accessed: 2024-12-12.
- [27] INSEE. Travail – origine–destination rp-mobpro 2015 (dbase). <https://www.insee.fr/fr/statistiques/3566008>, 2015. Accessed: 2024-12-12.
- [28] INSEE. Études – origine–destination rp-mobsco 2015 (dbase). <https://www.insee.fr/fr/statistiques/3565982>, 2015. Accessed: 2024-12-12.
- [29] INSEE. Répertoire des zones iris 2017 – fichier xls. <https://www.insee.fr/fr/information/2017499>, 2017. Accessed: 2024-12-12.
- [30] INSEE. Recensement des services et équipements (bpe 2019). <https://www.insee.fr/fr/statistiques/3568638>, 2019. Accessed: 2024-12-12.
- [31] Grzegorz Jamróz, Ahmet Onur Akman, Anastasia Psarou, Zoltán György Varga, and Rafał Kucharski. Social implications of coexistence of cavs and human drivers in the context of route choice. *Scientific Reports*, 15(1):6768, 2025.
- [32] Nishant Kheterpal, Eugene Vinitsky, Cathy Wu, Aboudy Kreidieh, Kathy Jang, Kanaad Parvate, and Alexandre Bayen. Flow: Open source reinforcement learning for traffic control. In *Proceedings of the 2nd Conference on Robot Learning (CoRL)*, 2018.
- [33] B. Ravi Kiran, Ilyes Sobh, Vincent Talpaert, Patrick Mannion, Ahmad Al Sallab, Senthil Yogamani, and Patrick Pérez. Deep reinforcement learning for autonomous driving: A survey. *IEEE Transactions on Intelligent Transportation Systems*, 23(6):4909–4926, 2022.
- [34] Daniel Krajzewicz, Jakob Erdmann, Michael Behrisch, and Laura Bieker. Recent development and applications of SUMO–simulation of urban mobility. *International Journal On Advances in Systems and Measurements*, 5(3&4):128–138, 2012.
- [35] Stefan Krauss. Microscopic modeling of traffic flow: Investigation of collision free vehicle dynamics. *Ph.D. Thesis, University of Cologne*, 1997.
- [36] Ken Ming Lee, Sriram Ganapathi Subramanian, and Mark Crowley. Investigation of independent reinforcement learning algorithms in multi-agent environments. *CoRR*, abs/2111.01100, 2021.

- [37] Silas C. Lobo, Stefan Neumeier, Evelio M. G. Fernandez, and Christian Facchi. Intas – the ingolstadt traffic scenario for sumo, 2020.
- [38] Pablo Alvarez Lopez, Michael Behrisch, Laura Bieker-Walz, Jakob Erdmann, Yun-Pang Flötteröd, Robert Hilbrich, Leonhard Lücken, Johannes Rummel, Peter Wagner, and Evamarie Wießner. Microscopic traffic simulation using sumo. In *The 21st IEEE International Conference on Intelligent Transportation Systems*. IEEE, 2018.
- [39] Ryan Lowe, Yi Wu, Aviv Tamar, Jean Harb, Pieter Abbeel, and Igor Mordatch. Multi-agent actor-critic for mixed cooperative-competitive environments. *CoRR*, abs/1706.02275, 2017.
- [40] Shu Lu and Yu Marco Nie. Stability of user-equilibrium route flow solutions for the traffic assignment problem. *Transportation Research Part B: Methodological*, 44(4):609–617, 2010.
- [41] Nina Mazyavkina, Sergey Sviridov, Sergei Ivanov, and Evgeny Burnaev. Reinforcement learning for combinatorial optimization: A survey. *Computers & Operations Research*, 134:105400, 2021.
- [42] McKinsey & Company. Autonomous vehicles: Moving forward—perspectives from industry leaders, 2023.
- [43] Ministry of Ecology (France). Enquête nationale transports et déplacements (entd 2008) – tableaux de données csv. <https://www.statistiques.developpement-durable.gouv.fr/enquete-nationale-transports-et-deplacements-entd-2008>, 2008. Accessed: 2024-12-12.
- [44] Anusha Nagabandi, Ignasi Clavera, Simin Liu, Ronald S. Fearing, Pieter Abbeel, Sergey Levine, and Chelsea Finn. Learning to adapt in dynamic, real-world environments through meta-reinforcement learning, 2019.
- [45] Kai Nagel and Gunnar Flötteröd. Agent-based traffic assignment: Going from trips to behavioural travelers. In *Travel Behaviour Research in an Evolving World—Selected papers from the 12th international conference on travel behaviour research*, pages 261–294. International Association for Travel Behaviour Research, 2012.
- [46] Hadi Nekoei, Akilesh Badrinaaraayanan, Amit Sinha, Mohammad Amini, Janarthanan Rajendran, Aditya Mahajan, and Sarath Chandar. Dealing with non-stationarity in decentralized cooperative multi-agent deep reinforcement learning via multi-timescale learning, 2023.
- [47] OpenStreetMap contributors. Planet dump retrieved from <https://planet.osm.org>. <https://www.openstreetmap.org>, 2024. Accessed: 2025-04-28.
- [48] Ling Pan, Tabish Rashid, Bei Peng, Longbo Huang, and Shimon Whiteson. Regularized softmax deep multi-agent q -learning, 2021.
- [49] Georgios Papoudakis, Filippos Christianos, Lukas Schäfer, and Stefano V. Albrecht. Benchmarking multi-agent deep reinforcement learning algorithms in cooperative tasks, 2021.
- [50] Anastasia Psarou, Ahmet Onur Akman, Łukasz Gorczyca, Michał Hoffmann, Zoltán György Varga, Grzegorz Jamróz, and Rafał Kucharski. Autonomous vehicles using multi-agent reinforcement learning for routing decisions can harm urban traffic. *arXiv preprint arXiv:2502.13188*, 2025.
- [51] Gabriel Ramos, Ana Bazzan, and Bruno da Silva. Analysing the impact of travel information for minimising the regret of route choice. *Transportation Research Part C: Emerging Technologies*, 88:257–271, 03 2018.
- [52] Tabish Rashid, Gregory Farquhar, Bei Peng, and Shimon Whiteson. Weighted QMIX: expanding monotonic value function factorisation. *CoRR*, abs/2006.10800, 2020.
- [53] Tabish Rashid, Mikayel Samvelyan, Christian Schroeder de Witt, Gregory Farquhar, Jakob Foerster, and Shimon Whiteson. QMIX: Monotonic Value Function Factorisation for Deep Multi-Agent Reinforcement Learning, 2018. Version Number: 2.

- [54] Wilko Schwarting, Alyssa Pierson, Javier Alonso-Mora, Sertac Karaman, and Daniela Rus. Social behavior for autonomous vehicles. *Proceedings of the National Academy of Sciences*, 116(50):24972–24978, 2019.
- [55] Steven E. Shladover. Connected and automated vehicle systems: Introduction and overview. *Journal of Intelligent Transportation Systems*, 22(3):190–200, 2018.
- [56] Zhenyu Shou, Xu Chen, Yongjie Fu, and Xuan Di. Multi-agent reinforcement learning for markov routing games: A new modeling paradigm for dynamic traffic assignment. *Transportation Research Part C: Emerging Technologies*, 137:103560, 2022.
- [57] Ming Tan. *Multi-agent reinforcement learning: independent vs. cooperative agents*, page 487–494. Morgan Kaufmann Publishers Inc., San Francisco, CA, USA, 1997.
- [58] J Terry, Benjamin Black, Nathaniel Grammel, Mario Jayakumar, Ananth Hari, Ryan Sullivan, Luis S Santos, Clemens Dieffendahl, Caroline Horsch, Rodrigo Perez-Vicente, Niall Williams, Yashas Lokesh, and Praveen Ravi. Pettingzoo: Gym for multi-agent reinforcement learning. In M. Ranzato, A. Beygelzimer, Y. Dauphin, P.S. Liang, and J. Wortman Vaughan, editors, *Advances in Neural Information Processing Systems*, volume 34, pages 15032–15043. Curran Associates, Inc., 2021.
- [59] Luiz A Thomasini, Lucas N Alegre, Gabriel de O Ramos, and Ana LC Bazzan. Routechoiceenv: a route choice library for multiagent reinforcement learning. In *Adaptive and Learning Agents Workshop (ALA 2023) at AAMAS, London, UK*, volume 2023, 2023.
- [60] Martin Treiber, Ansgar Hennecke, and Dirk Helbing. Congested traffic states in empirical observations and microscopic simulations. *Physical Review E*, 62(2):1805–1824, August 2000.
- [61] Kagan Tumer and Adrian Agogino. Agent reward shaping for alleviating traffic congestion. In *Workshop on agents in traffic and transportation*, volume 87. Citeseer, 2006.
- [62] Tze-Yang Tung, Szymon Kobus, Joan Pujol Roig, and Deniz Gündüz. Effective communications: A joint learning and communication framework for multi-agent reinforcement learning over noisy channels. *IEEE Journal on Selected Areas in Communications*, 39(8):2590–2603, 2021.
- [63] Eugene Vinitsky, Aboudy Kreidieh, Luc Le Flem, Nishant Kheterpal, Kathy Jang, Cathy Wu, Fangyu Wu, Richard Liaw, Eric Liang, and Alexandre M. Bayen. Benchmarks for reinforcement learning in mixed-autonomy traffic. In *Proceedings of The 2nd Conference on Robot Learning*, pages 399–409. PMLR, 2018.
- [64] Tonghan Wang, Heng Dong, Victor R. Lesser, and Chongjie Zhang. ROMA: multi-agent reinforcement learning with emergent roles. *CoRR*, abs/2003.08039, 2020.
- [65] J G Wardrop. ROAD PAPER. SOME THEORETICAL ASPECTS OF ROAD TRAFFIC RESEARCH. *Proceedings of the Institution of Civil Engineers*, 1(3):325–362, May 1952.
- [66] World Economic Forum. Autonomous vehicles: Timeline and roadmap ahead, 2025.
- [67] Lixuan Wu, Zhongxiang Huang, Jianhui Wu, Zhibo Gao, and Dingming Qin. A Day-to-Day Stochastic Traffic Flow Assignment Model Based on Mixed Regulation. *IEEE Access*, 8:12815–12823, 2020.
- [68] Chao Yu, Akash Velu, Eugene Vinitsky, Jiaxuan Gao, Yu Wang, Alexandre Bayen, and Yi Wu. The surprising effectiveness of ppo in cooperative, multi-agent games, 2022.
- [69] Chongjie Zhang and Victor Lesser. Coordinating multi-agent reinforcement learning with limited communication. In *Proceedings of the 2013 international conference on Autonomous agents and multi-agent systems*, pages 1101–1108, 2013.
- [70] Lei Zhang and David Levinson. Agent-based approach to travel demand modeling: Exploratory analysis. *Transportation Research Record*, 1898(1):28–36, 2004.
- [71] Meng Zhou, Ziyu Liu, Pengwei Sui, Yixuan Li, and Yuk Ying Chung. Learning implicit credit assignment for multi-agent actor-critic. *CoRR*, abs/2007.02529, 2020.

- [72] Yihe Zhou, Shunyu Liu, Yunpeng Qing, Kaixuan Chen, Tongya Zheng, Yanhao Huang, Jie Song, and Mingli Song. Is centralized training with decentralized execution framework centralized enough for marl?, 2023.

Appendix

Appendix	15
A Data: Networks and travel demand	15
B Experiment details and reproducibility	16
C Accessibility and usage	17
D Components and dependencies	19
E Demand statistics and network layouts	22
F Supplementary results	25

A Data: Networks and travel demand

A.1 Synthetic population with travel demand in Île-de-France networks

To ensure our agents operate within a highly realistic setting, we generated a synthetic population and its travel demand following the methodology of Hörl and Balac[22]. Their framework leverages publicly accessible datasets and open-source code ³, ensuring that simulation inputs can be fully reproduced. It utilizes very detailed French statistical data, which consists of granular information on individual attributes and travel behaviors.

The synthetic-population generation proceeded through four main stages:

1. Population Synthesis.

We began by matching 30% microsample census data (covering disaggregated data on persons and households [26]) with population counts and characteristics for each spatial unit in Île-de-France ([25], [23], [29]). Households were replicated until the region’s 12 million inhabitants were properly represented in each area. In the end, each synthetic individual had demographic attributes (age, sex, socio-professional category, employment or education status) as well as household characteristics (household size, number of vehicles, and home location in the specific area).

2. Activity-Trip Enrichment.

Next, we assigned each person a full-day activity schedule and trip chain drawn from the national household travel survey ([43]). Using a statistical-matching procedure, we paired synthetic individuals with the survey’s disaggregated records based on discrete attribute similarity (e.g., age group, sex), thereby transferring realistic activity–trip patterns to each agent.

3. Primary Location Allocation.

For each household, a random home address location was sampled within its spatial zone ([24]). We then assigned workplaces to employed agents to reconcile the census-derived inter-zonal commuting matrix ([27]), enterprise locations weighted by number of employees ([12]), and the individual’s target commute distance (inferred from their trip chain). Educational institutions were similarly allocated for students ([28]), drawing upon the national Service and Facility database ([30]).

4. Secondary Activity Assignment.

Finally, secondary purposes (leisure, shopping, and other activities) were allocated using the approach of Hörl and Axhausen ([21]), which accounts for each agent’s primary activities, proximity to service and facility locations, and matching inter-site distances along with the activity chain distances.

³<https://github.com/eqasim-org/ile-de-france/tree/v1.2.0>

This procedure yielded synthetic trip data for the Île-de-France region, within which we selected inner trips in 28 subregions. This data is formatted as CSV files, each row describing a single trip made by an individual and consisting of 21 attributes of each trip, including: `person_id`, `trip_index`, `departure_time`, `arrival_time`, `preceding_purpose`, `following_purpose`, `ox`, `oy`, `dx`, `dy`, `abm_region`, ... where `(ox, oy)` and `(dx, dy)` are coordinates of the trip origin and destination.

We then converted this raw trip data into a format compatible with RouteRL using the processing pipeline described below.

1. **Demand filtering** For each region, trips are filtered according to their departure times by a predefined time window. For managing the computation time of our experiments, we set it to be a half-hour time period starting from 9 AM.
2. **Network extraction** For each region, the corresponding OpenStreetMap file extract is converted to SUMO network files (`*.nod.xml`, `*.edg.xml`, `*.con.xml`, `*.net.xml`, `*.rou.xml`, `*.tll.xml`, `*.typ.xml`) using `netconvert`. Non-passenger edges are eliminated.
3. **Edge mapping** Origin and destination coordinates are snapped to the nearest traversable edge midpoint, computed from node coordinates. Trips whose origin or destination corresponds to an isolated or dead-end edge are discarded.
4. **Route generation** For a trip to be used in route choice, we must be able to generate multiple routes between its origin and destination. Not all trips satisfied this condition. Therefore, we then filter out trips whose origin and destination cannot be connected to up to 4 routes by JanuX [1], which is the custom route generation tool, also used in RouteRL.
5. **Output files**
 - **Agent metadata** (`agents.csv`): List of agents where each have ID, origin, destination, and departure time used in the simulations.
 - **Network files**: XML files ready to be loaded by SUMO.

With URB, we make the raw trip data⁴ and the converted URB-usable network-demand dataset⁵ publicly available for general use.

A.2 Processing of InTAS Ingolstadt data from RESCO

We used one of the well-established SUMO scenarios, already utilized in RESCO traffic-light benchmark[4], namely “InTAS” [37]. It describes traffic within a real-world city, Ingolstadt (Germany), including road network layout and calibrated demands.

The demand in RESCO was static; thus we needed to convert it. We used the same trip demand as in the original dataset, yet converted each trip (vehicle assigned to a route at a given departure) to the request (origin, destination, and departure time). Then, we sampled four routes for each unique OD pair with JanuX [1] and filtered out OD pairs with fewer possible routes. Finally, we selected trips within a half-hour period for computational efficiency. The resulting data (demand and network files) are provided within the same dataset as the Île-de-France data (see Appendix A.1). The script⁶ used for this processing pipeline is publicly available in a public repository.

B Experiment details and reproducibility

Code. All experimental results reported in this paper are created using the scripts and the configuration files included in URB’s public GitHub repository.

Results data. All results produced in the experiments reported in this paper are stored and made publicly available on a separate GitHub repository⁷. This repository contains subdirectories that classify different experimental settings and is organized as listed in Table 2.

⁴<https://doi.org/10.34740/kaggle/ds/7302756>

⁵<https://doi.org/10.34740/kaggle/ds/7406751>

⁶https://github.com/COEXISTENCE-PROJECT/extract_resco_demand

⁷https://github.com/COEXISTENCE-PROJECT/URB_data

Table 2: Directory organization of publicly available experiment data.

Directory name	Experiment	Reported in
scenario1	40% CAVs	Figure 3 and Table 1
scenario1_long	40% CAVs (long training)	Figure 3 (triangular markers)
scenario2	100% CAVs	Figure 4
demonstrative	Demonstrative	Figure 9
hyperparam_search	Hyperparameter tuning	-

Parameterization. Each experiment’s data is organized within a dedicated directory in the above-mentioned dedicated GitHub repository, semantically named after the used network, algorithm, and seed value. Each of these folders includes a `exp_config.json` file, which stores all the parameterization used in that particular experiment. We refer the interested reader to these configuration files to ensure the reproducibility of our experiments.

Hardware and compute time. Our experiments are conducted on our institution’s computing nodes with resources allocated as listed in Table 3. Experiment compute time is highly dependent on the simulated scenario and parameterization. We share the computation time of 4 representative cases in Table 4.

Table 3: Summary of computational environment used for experiments.

Component	Specification
CPU	Intel(R) Xeon(R) Gold 5122 CPU, 3.60GHz
GPU	NVIDIA GeForce RTX 2080
RAM	64 GB allocated per job
Operating system	Ubuntu 24.04.1 LTS
Job scheduler	SLURM
SUMO version	1.18.0

Table 4: Computation time of four representative experiments. The first three experiments are run for 200 human learning and 6000 CAV training episodes (test phase omitted) with 40% CAVs. The last experiment is run for 200 human learning and 300 baseline running episodes for 40% CAVs.

Traffic network	Algorithm	Runtime (hours)
St. Arnoult	QMIX	~15.5
Provins	QMIX	~44
Ingolstadt	QMIX	~152.5
Ingolstadt	AON (Baseline)	~4.25

Overall, the experiments described in the paper required approximately 4,000 hours of computation, distributed across multiple concurrent environments. Full research required up to twice as much computation in total, due to preliminary testing, errors, and our curiosity-driven exploration.

C Accessibility and usage

C.1 Licensing and availability

Our code and the input data are released under the MIT License. The code, the datasets, and the documentation on how to use URB are publicly available in the GitHub repository⁸. The datasets (networks and travel demand) are also released under the MIT License. All data for creating the benchmarking environment and task scenarios are based on publicly available open data. SUMO

⁸<https://github.com/COEXISTENCE-PROJECT/URB>

traffic simulator is licensed under the EPL-2.0 with GPL v2 or later as a secondary license option (refer to SUMO website⁹ for more details).

C.2 Quickstart: Code Ocean capsule

For a quick start on interaction with URB, we provide an executable code capsule at Code Ocean¹⁰ that executes a concise demonstrative experiment using the QMIX algorithm in the St. Arnoult network. This environment comes with all dependencies (including SUMO) preinstalled, allowing the experiment to be reproduced with a single click via the *Reproducible Run* feature. We invite interested readers to explore this capsule to examine the experimental workflow and output formats in a fully isolated and controlled setting.

C.3 Installation and usage

Mind that SUMO must be installed and available on the system. This procedure should be carried out separately¹¹.

Clone the URB repository from GitHub:

```
git clone https://github.com/COEXISTENCE-PROJECT/URB.git
```

Create a virtual environment with `venv`:

```
python -m venv .venv
```

then install the dependencies:

```
cd URB
pip install -r requirements.txt
```

or use a conda environment:

```
conda create -n URB python=3.13.1
```

and then install the dependencies:

```
cd URB
conda activate URB
pip install -r requirements.txt
```

To use URB with a reinforcement learning algorithm, run the following command:

```
python scripts/<script_name> --id <exp_id> --alg-conf <hyperparam_id>
--env-conf <env_conf_id> --task-conf <task_id> --net <net_name>
--env-seed <env_seed> --torch-seed <torch_seed>
```

Where:

- `<script_name>` points to the algorithm implementation (provided TorchRL scripts, or the user's implementation). Provided MARL training scripts include: `ippo_torchrl`, `iq1_torchrl`, `mappo_torchrl`, `qm1x_torchrl`, or `vdn_torchrl.py`.
- `<id>` is the unique experiment identifier, which can be any string and is used to organize the training records and metrics alongside other experiments (e.g., `vdn_malicious_ingolstadt`).
- `<hyperparam_id>` is the algorithm hyperparameter configuration. It must correspond to a JSON filename (without extension) in `config/alg1_config` directory. Provided scripts automatically select the algorithm-specific subfolder in this directory. Users can add their custom parameterizations by following the structure of the provided ones and use them similarly.

⁹<https://eclipse.dev/sumo/>

¹⁰<https://codeocean.com/capsule/1896262/tree>

¹¹Instructions available at: <https://sumo.dlr.de/docs/Installing/index.html>

- `<env_conf_id>` is the environment configuration identifier. It must correspond to a JSON filename (without extension) in `config/env_config` directory. It is used to parameterize environment-specific processes, such as path generation, disk operations, etc. It is **optional** and by default is set to `config1`. Users can add their custom environment settings by following the structure of the provided ones and using them similarly.
- `<task_id>` is the task configuration identifier. It must correspond to a JSON filename (without extension) in `config/task_config` directory. It is used to parameterize the simulated scenario, such as a portion of CAVs, duration of human learning, CAV behavior, etc. Users can define custom tasks by following the structure of the provided definitions and use them similarly.
- `<net_name>` is the network graph and corresponding demand pattern. It must correspond to one of the subdirectory names in `networks/`. We provide all the networks used in this paper (`gretz_armainvilliers`, `ingolstadt_custom`, `nangis`, `nemours`, `provins`, and `saint_arnoult`) in this directory. Users can download the network of their choice from our dataset on Kaggle and place it in this directory, then use it similarly.
- `<env_seed>` is the seed for the traffic environment (default: 42).
- `<torch_seed>` is the seed for PyTorch (default: 42).

Example:

```
python scripts/qmix_torchrl.py --id sai_qmix_0 --alg-conf config3 --
task-conf config4 --net saint_arnoult --env-seed 42 --torch-seed
0
```

Results and plots will be saved in `results/<exp_id>`.

To run baseline models, use the following command (notice the additional `-model` flag instead of `-torch-seed`):

```
python scripts/baselines.py --id <exp_id> --alg-conf <hyperparam_id>
--env-conf <configuration_id> --task-conf <task_id> --net <
net_name> --env-seed <env_seed> --model <model_name>
```

Where `<model_name>` is one of: `aon`, `random` (baseline models included in URB, under `baseline_models/`), or `gawron` (a human learning model from RouteRL).

Example:

```
python scripts/baselines.py --id ing_aon --alg-conf config1 --task-
conf config2 --net ingolstadt_custom --model aon
```

C.4 Access to networks

We include only six traffic networks and associated demand data (Gretz-Armainvilliers, Ingolstadt, Nangis, Nemours, Provins, Saint-Arnoult) in URB’s GitHub repository for the sake of saving the repository space. Users who wish to utilize the entire URB network and demand library can (1) download corresponding network folders from URB’s Kaggle data repository, (2) place the network folder in the `networks/` directory, (3) use via the `-net` flag as described above.

D Components and dependencies

D.1 RouteRL

To study the routing behavior of CAVs in complex urban environments, we rely on RouteRL [2], an open-source framework that couples MARL with microscopic traffic simulation. RouteRL is designed to model daily route choices of heterogeneous driver agents, including both human drivers, emulated using behaviorally grounded models, and CAVs, modeled as MARL agents optimizing routing strategies based on predefined objectives such as travel time or system efficiency. The framework supports flexible experimentation through configurable traffic networks, CAV market shares, routing algorithms, and behavioral heterogeneity.

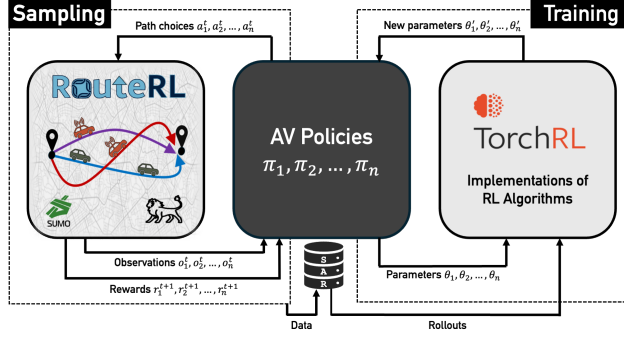


Figure 5: Reproduced from Figure 2 in [2]. **A typical multi-agent training pipeline using RouteRL:** The training procedure alternates between two stages: (i) *Sampling* (left), where the traffic microsimulator (SUMO) returns rewards resulting from given route choices made by all agents, and (ii) *Training* (right), where the collected experiences are used to train CAV policies via TorchRL’s MARL algorithm implementations. Policy parameters are iteratively updated and fed back into the sampling loop.

D.2 SUMO

We use the Simulation of Urban MObility (SUMO) [34, 6] as the underlying microscopic traffic simulator to model realistic traffic dynamics in urban environments. SUMO is an open-source, highly portable, and extensible platform designed to simulate the movement of individual vehicles based on time-continuous, space-continuous traffic flow models. Its core simulation engine models vehicle behavior using the Krauss car-following model [35], which includes stochastic acceleration, deceleration, and gap-keeping behavior to capture real-world driving variability. Lane-changing is handled through a rule-based model that accounts for safety, convenience, and strategic routing decisions. SUMO supports loading real-world road networks (e.g., from OpenStreetMap), making it ideal for simulations in large-scale, realistic urban scenarios. Each vehicle can be treated as an agent, with states defined by observable traffic variables (e.g., position, speed, headway) and actions corresponding to routing choices or lane changes. The simulator provides a high-frequency, low-latency API (TraCI) that enables real-time communication between the RL agent and the simulation environment. This allows agents to receive observations, perform actions, and obtain reward signals in a closed loop.

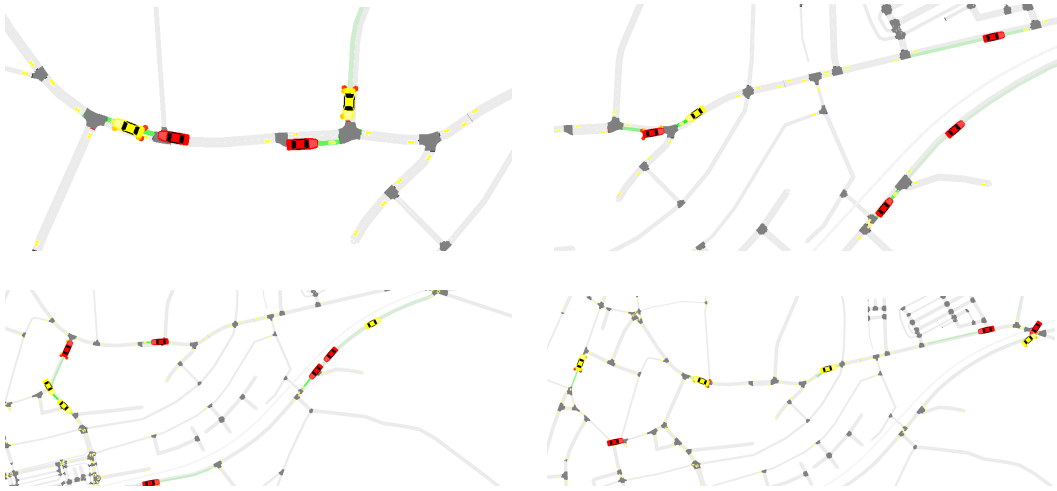


Figure 6: Screenshots from SUMO GUI, from an experiment conducted using the Provins traffic network. Yellow vehicles represent CAVs, while red vehicles indicate human drivers. Junctions are shown with dark grey, and yellow rectangles represent traffic detectors.

D.3 Human learning model - day-to-day agent-based route choice model

Learning Human agent i updates expected travel time $\bar{C}_{i,\tau,k}$ every day τ on the selected route k , based on the actual travel time $\hat{C}_{i,j,k}$ experienced in the earlier days j . The update, with a learning rate α_0 , occurs only if the difference between the expected and experienced travel times exceeds the bounded rationality threshold γ_C . Each day j of recorded history τ is weighted with α_j :

$$\bar{C}_{i,\tau,k} = \begin{cases} \bar{C}_{i,\tau-1,k} & \text{if } a(i, \tau-1) \neq k \\ \begin{cases} \bar{C}_{i,\tau-1,k} & \text{if } |\bar{C}_{i,\tau-1,k} - \hat{C}_{i,\tau,k}| \leq \gamma_C \\ \alpha_0 * \bar{C}_{i,\tau-1,k} + \sum_{j=0}^{\tau-1} \alpha_j * \hat{C}_{i,j,k} & \text{if } a(i, \tau-1) = k \end{cases} & \end{cases} \quad (1)$$

Agents' decision process - act Based on the expected costs \bar{C} learned so far, each agent selects a subjectively optimal route $a(i, \tau)$ following a utility maximization model. We model this behaviour by adding a random variable ε to the cost which is multiplied with β (to control the bias of the decisions):

$$U_{i,\tau,k} = \beta \bar{C}_{i,\tau,k} + \varepsilon \quad (2)$$

where $\varepsilon = w_i * \varepsilon_i + w_{i,k} * \varepsilon_{i,k} + W_{i,k,\tau} * \varepsilon_{i,k,\tau}$ and

$$a(i, \tau) = \begin{cases} a(i, \tau-1) & \text{if } |\bar{C}_{i,\tau-1,k} - \bar{C}_{i,\tau,k}| \leq \gamma_u \\ \begin{cases} \arg \max_{k \in K_{OD}} U_{i,\tau,k} & \text{with prob. } 1 - \delta \\ \text{random choice} & \text{with prob. } \delta \end{cases} & \text{otherwise} \end{cases} \quad (3)$$

Remark: While RouteRL allows complex human models covering many empirically observed behaviours, such as heterogeneous agents, many parameter sets yielded unstable results. Therefore we opted for a simple model with $\gamma_C = 0$, $\gamma_u = 0$, $\varepsilon = 0$ and $\delta = 0$, which boils down to:

$$\bar{C}_{i,\tau,k} = \begin{cases} \bar{C}_{i,\tau-1,k} & \text{if } a(i, \tau-1) \neq k \\ 0.8 * \bar{C}_{i,\tau-1,k} + 0.2 * \hat{C}_{i,\tau-1,k} & \text{if } a(i, \tau-1) = k \end{cases} \quad (4)$$

and

$$a(i, \tau) = \arg \min_k \bar{C}_{i,\tau,k}.$$

The initial conditions are specified by $\bar{C}_{i,0,k}$ being the free flow travel time via route k which is computed from the network graph description generated by Open Street Map.

D.4 Route generation

For each agent, the action space is the discrete route options that connect their origins to their destinations and are precomputed. Agents with the same origin and destinations have the same action space. The action space sizes (i.e., number of routes) are the same for all agents and are determined by the parameter `number_of_paths` in the environment configuration, along with other path generation-related parameters. In all experiments reported in this paper, we set this value to 4 and it is used to set `path_generation_parameters/number_of_paths` in RouteRL's environment initialization¹². The parameters used for path generation are stored in the `exp_config.json` in the dedicated directory for each experiment in our public experiment data repository (See Appendix B for details).

Path generation procedure is managed by RouteRL and carried out by JanuX [1], the NetworkX-compatible path generation tool. For a given traffic network and user parameters, JanuX runs a modified Dial-like [15] algorithm-based process to sample the desired number of paths with desired characteristics. Paths generated for 4 example origin-destination pairs in Ingolstadt, Provins, and St. Arnould traffic networks are depicted in Figure 7.

¹²For details about RouteRL's parameterization scheme: https://coexistence-project.github.io/RouteRL/documentation/pz_env.html

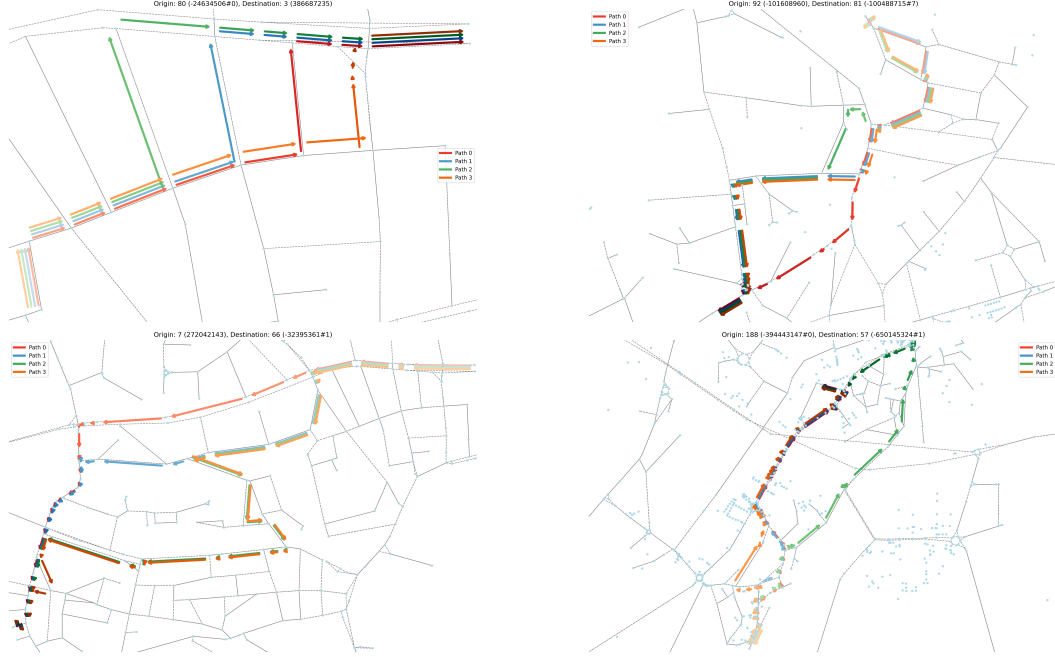
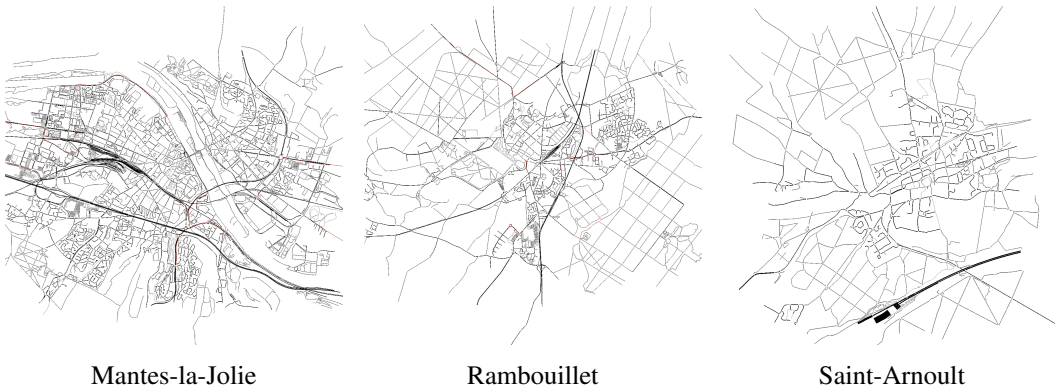


Figure 7: Routes generated for 4 selected origin-destination pairs in 3 different traffic networks used in our experiments (Ingolstadt (left), St. Arnoult (top right), Provins (bottom right)). Each shading color represents a different route.

E Demand statistics and network layouts

For each traffic network included in URB, Table 5 shows the number of trips and the number of unique origin-destination pairs in the demand data. The network layouts are depicted in Figure 8.





Étampes



Souppes-sur-Loing



Nemours



Fontainebleau



Montereau-Fault-Yonne



Nangis



Provins



Coulommiers



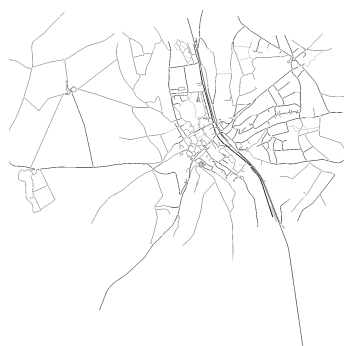
Meaux



La Ferté



Othis



Maule



Beynes



Parmain



Gargenville



Melun



Ozoir-la-Ferrière



Gretz-Armainvilliers



La Verrière



Guyancourt



Plaisir



Bussy-Saint-Georges



Fontenay-en-Parisis



Les Mureaux

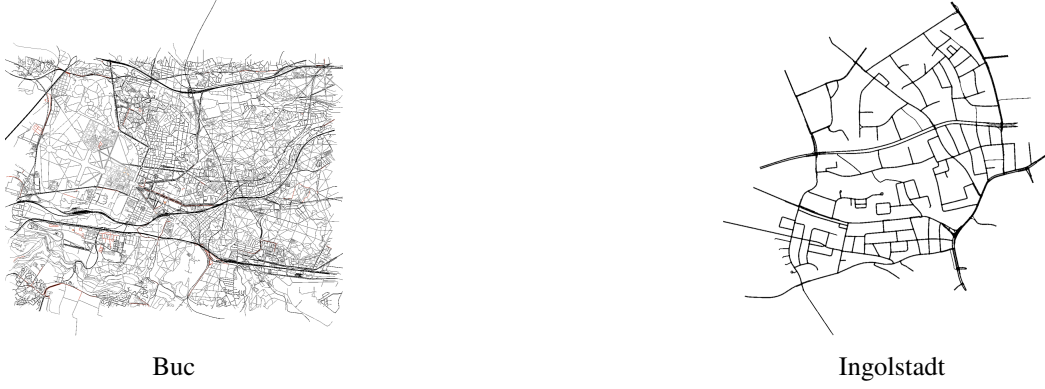


Figure 8: All 29 traffic networks included in URB. First 28 networks are from subregions of Île-de-France, and the last network, Ingolstadt, is imported from RESCO [4].

Table 5: The number of trips and unique origin-destinations in the demand per region.

Region	Number of trips	Unique OD pairs
Mantes-la-Jolie	4271	4143
Rambouillet	1507	1450
Saint-Arnoult	222	215
Étampes	1159	1124
Souppes-sur-Loing	205	204
Nemours	729	724
Fontainebleau	1352	1325
Montereau-Fault-Yonne	778	761
Nangis	362	352
Provins	523	517
Coulommiers	549	542
Meaux	2637	2590
La Ferté	269	267
Othis	841	830
Maule	225	221
Beynes	234	229
Parmain	761	753
Gargenville	1000	960
Melun	4107	4054
Ozoir-la-Ferrière	643	633
Gretz-Armainvilliers	636	629
La Verrière	3521	3431
Guyancourt	2405	2352
Plaisir	1924	1867
Bussy-Saint-Georges	724	714
Fontenay-en-Parisis	2068	2018
Les Mureaux	2112	2049
Buc	6924	6791
Ingolstadt	1035	306

F Supplementary results

F.1 Performance metrics for Scenario 2

Table 6 reports the performance indicators for our experiments in Scenario 2 (as introduced in Section 4).

Table 6: Performance metrics for 4 MARL algorithms in Scenario 2 (100% of vehicles are CAVs) in the St. Arnould network. The best results from 3 runs of the CAV travel times are reported. As in Scenario 1, the CAVs experience a longer travel time t than in the human-only system. The training costs c are significant for all the instances, and overall network performance decreased (lower speed: $\Delta_V < 0$ and increased mileage: $\Delta_L > 0$). This shows, that even in simpler case - without competition with human agents, there is place for improvement. The best result for each metric is **bolded**.

NET	ALGORITHM	t^{PRE}	t^{TEST}	t_{CAV}	t_{HDV}	c_{ALL}	c_{HDV}	c_{CAV}	Δ_V	Δ_L	WR
ST. ARNOULT	IPPO	3.15	3.51	3.51	N/A	1.65	0.0	1.65	-0.76	0.15	0%
	IQL	3.15	3.64	3.64	N/A	0.37	0.0	0.37	-0.6	0.21	0%
	MAPPO	3.15	3.65	3.65	N/A	0.65	0.0	0.65	-0.7	0.21	0%
	QMIX	3.15	3.58	3.58	N/A	0.42	0.0	0.42	-0.63	0.18	0%
	HUMAN	3.15	3.15	N/A	3.15	0.0	0.0	0.0	0.0	0.0	100%
	AON	3.15	3.09	3.09	N/A	0.17	0.0	0.17	0.03	-0.1	100%
	RANDOM	3.15	3.65	3.65	N/A	0.72	0.0	0.72	-0.83	0.19	0%

F.2 Demonstrative experiments

To further showcase URB’s flexibility and capabilities, we complement the results reported in this paper with three demonstrative experiments:

- **Selfish CAVs versus adapting humans in Nangis:** In **Nangis**, what happens when the **40%** of the drivers convert into **selfish** CAVs, who thereafter learn routing strategies with the **IPPO** algorithm while the remaining humans are simultaneously **adapting** to these changes?
- **Malicious CAVs in Nemours:** In **Nemours**, what happens when the **40%** of the drivers convert into **malicious** CAVs, who learn to maximize negative impact for humans, with the **QMIX** algorithm?
- **Altruistic CAVs in Gretz-Armainvilliers:** In **Gretz-Armainvilliers**, what happens when the **40%** of the drivers convert into **altruistic** CAVs, who aim to improve overall traffic efficiency, with the **VDN** algorithm, while the remaining humans are simultaneously **adapting** to these changes?

The experiment results, conducted with parameterization shared in our result data repository as described in Appendix B, are provided in Figure 9.

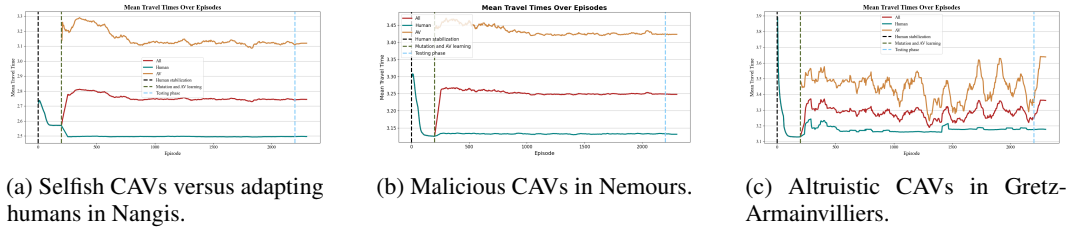
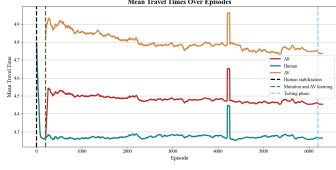


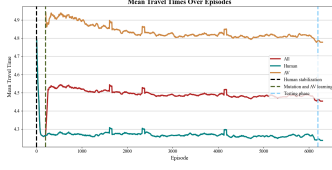
Figure 9: Mean travel times (in minutes) of humans and CAVs over the episodes in demonstrative experiments.

F.3 Additional plots: Travel times across episodes

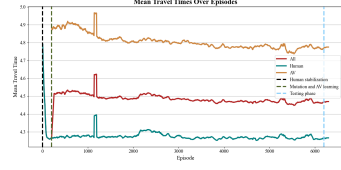
By default, at the end of each URB experiment, several plots are generated using RouteRL’s built-in plotting functions. These visualizations can be a starting point for analyses and are excellent for early detection of potential issues. In this section, we share the plots for travel time changes produced for the experiments reported in Section 4, including all repetitions.



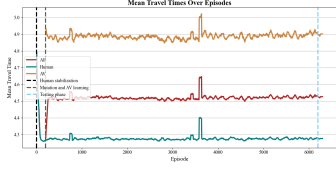
Scenario 1, Ingolstadt, IPPO, torch seed 0



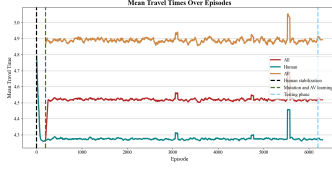
Scenario 1, Ingolstadt, IPPO, torch seed 1



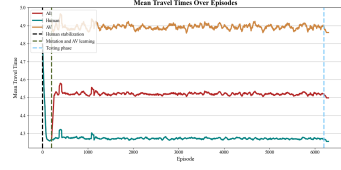
Scenario 1, Ingolstadt, IPPO, torch seed 2



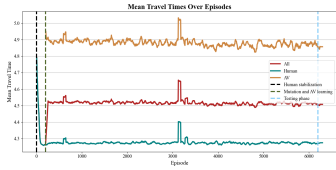
Scenario 1, Ingolstadt, MAPPO, torch seed 0



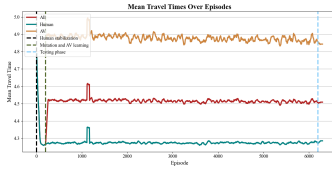
Scenario 1, Ingolstadt, MAPPO, torch seed 1



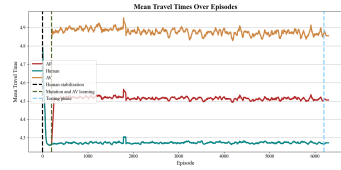
Scenario 1, Ingolstadt, MAPPO, torch seed 2



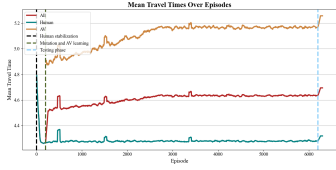
Scenario 1, Ingolstadt, IQL, torch seed 0



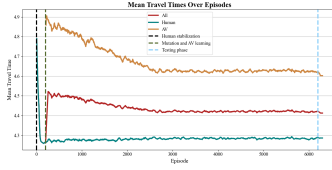
Scenario 1, Ingolstadt, IQL, torch seed 1



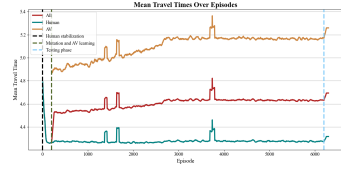
Scenario 1, Ingolstadt, IQL, torch seed 2



Scenario 1, Ingolstadt, QMIX, torch seed 0



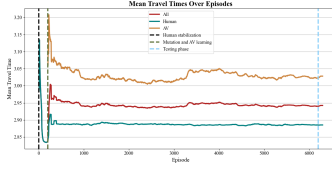
Scenario 1, Ingolstadt, QMIX, torch seed 1



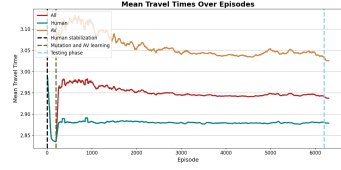
Scenario 1, Ingolstadt, QMIX, torch seed 2



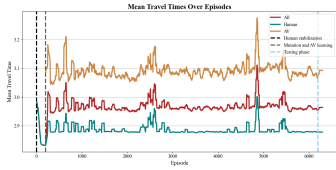
Scenario 1, Provins, IPPO, torch seed 0



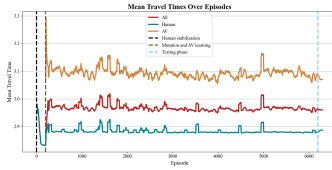
Scenario 1, Provins, IPPO, torch seed 1



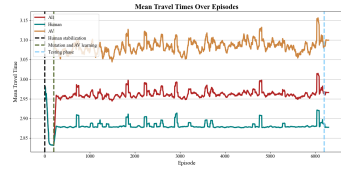
Scenario 1, Provins, IPPO, torch seed 2



Scenario 1, Provins, MAPPO, torch seed 0



Scenario 1, Provins, MAPPO, torch seed 1



Scenario 1, Provins, MAPPO, torch seed 2



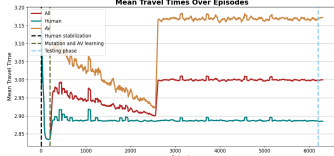
Scenario 1, Provins, IQL, torch seed 0



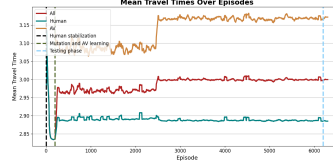
Scenario 1, Provins, IQL, torch seed 1



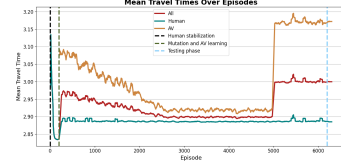
Scenario 1, Provins, IQL, torch seed 2



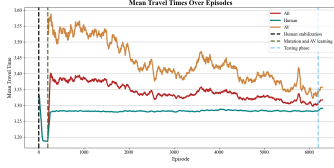
Scenario 1, Provins, QMIX, torch seed 0



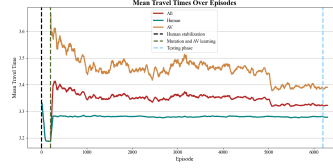
Scenario 1, Provins, QMIX, torch seed 1



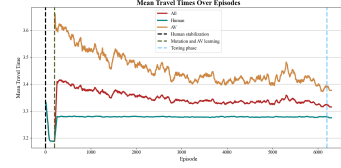
Scenario 1, Provins, QMIX, torch seed 2



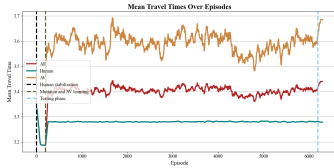
Scenario 1, Saint Arnault, IPPO, torch seed 0



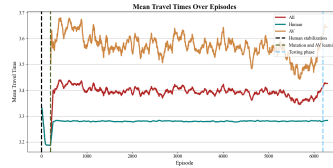
Scenario 1, Saint Arnault, IPPO, torch seed 1



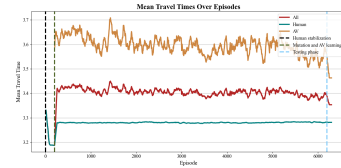
Scenario 1, Saint Arnault, IPPO, torch seed 2



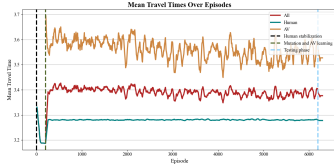
Scenario 1, Saint Arnault, MAPPO, torch seed 0



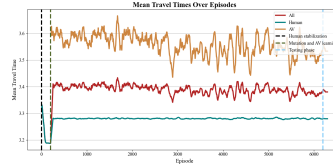
Scenario 1, Saint Arnault, MAPPO, torch seed 1



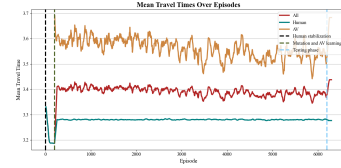
Scenario 1, Saint Arnault, MAPPO, torch seed 2



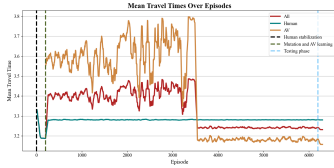
Scenario 1, Saint Arnault, IQL, torch seed 0



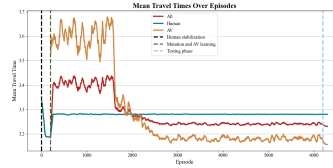
Scenario 1, Saint Arnault, IQL, torch seed 1



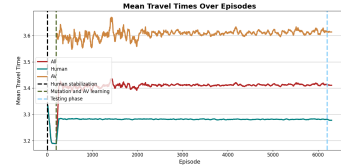
Scenario 1, Saint Arnault, IQL, torch seed 2



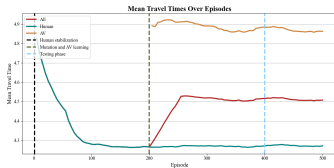
Scenario 1, Saint Arnault, QMIX, torch seed 0



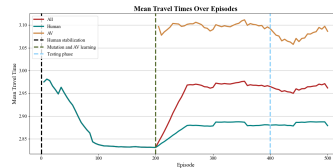
Scenario 1, Saint Arnault, QMIX, torch seed 1



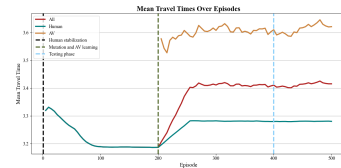
Scenario 1, Saint Arnault, QMIX, torch seed 2



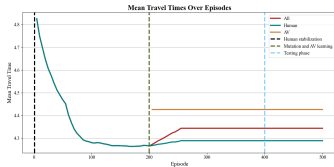
Scenario 1, Ingolstadt, Random baseline



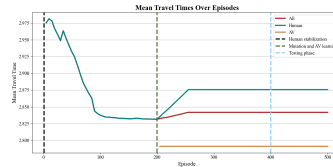
Scenario 1, Provins, Random baseline



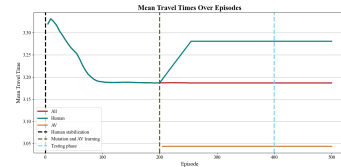
Scenario 1, Saint Arnault, Random baseline



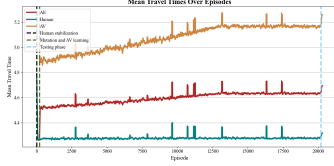
Scenario 1, Ingolstadt, AON baseline



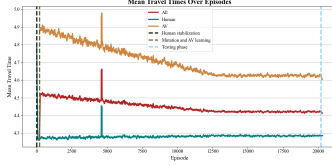
Scenario 1, Provins, AON baseline



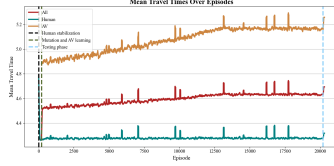
Scenario 1, Saint Arnault, AON baseline



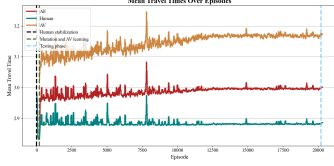
Scenario 1 (long), Ingolstadt, QMIX, torch seed 0



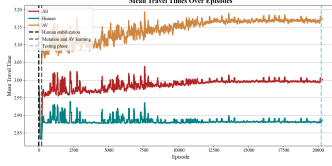
Scenario 1 (long), Ingolstadt, QMIX, torch seed 1



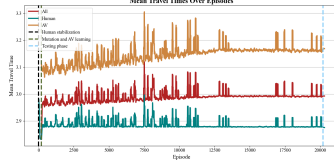
Scenario 1 (long), Ingolstadt, QMIX, torch seed 2



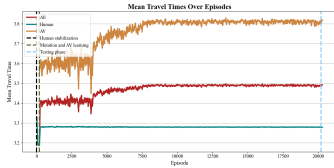
Scenario 1 (long), Provins, QMIX, torch seed 0



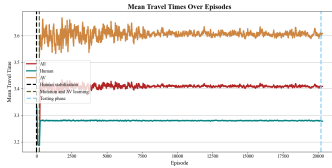
Scenario 1 (long), Provins, QMIX, torch seed 1



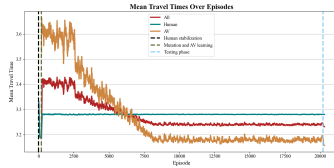
Scenario 1 (long), Provins, QMIX, torch seed 2



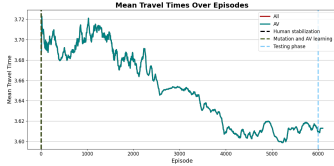
Scenario 1 (long), Saint Arnould, QMIX, torch seed 0



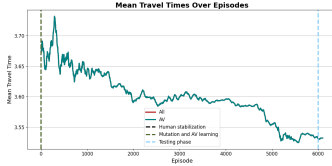
Scenario 1 (long), Saint Arnould, QMIX, torch seed 1



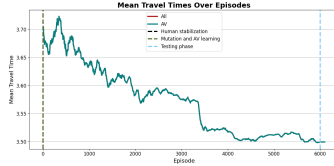
Scenario 1 (long), Saint Arnould, QMIX, torch seed 2



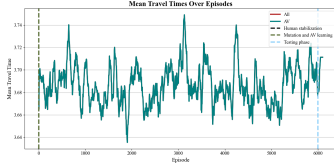
Scenario 2, Saint Arnould, IPPO, torch seed 0



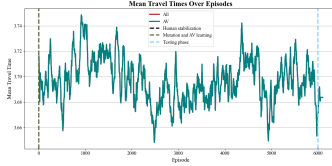
Scenario 2, Saint Arnould, IPPO, torch seed 1



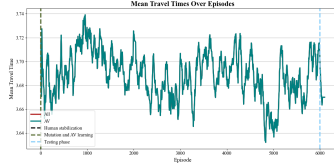
Scenario 2, Saint Arnould, IPPO, torch seed 2



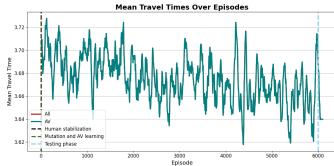
Scenario 2, Saint Arnould, MAPPO, torch seed 0



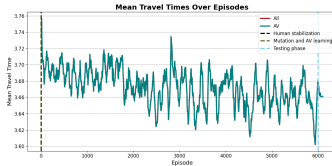
Scenario 2, Saint Arnould, MAPPO, torch seed 1



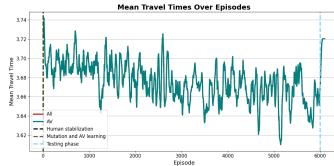
Scenario 2, Saint Arnould, MAPPO, torch seed 2



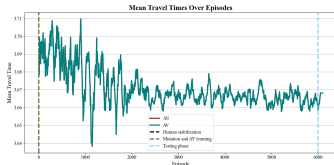
Scenario 2, Saint Arnould, IQL, torch seed 0



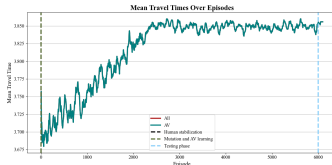
Scenario 2, Saint Arnould, IQL, torch seed 1



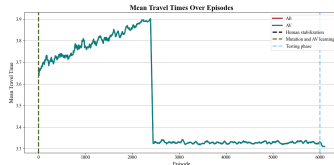
Scenario 2, Saint Arnould, IQL, torch seed 2



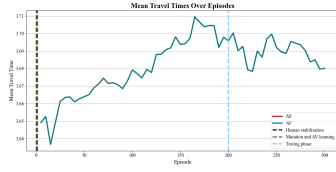
Scenario 2, Saint Arnould, QMIX, torch seed 0



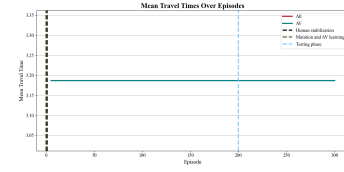
Scenario 2, Saint Arnould, QMIX, torch seed 1



Scenario 2, Saint Arnould, QMIX, torch seed 2



Scenario 2, Saint Arnould, Random baseline



Scenario 2, Saint Arnould, AON baseline

Figure 10: Travel times across episodes for all experiments reported in this study.